

Evaluating subgrade dynamic and static resilience modulus through enhanced testing techniques

Naitian Zhang^a, Peng Wang^b, Chengdong Xia^{c,d,*}, Lin Gao^b, Yongze Wang^b, Songtao Lv^c, Wang Dikuan^c

^a Xinjiang Key Laboratory of Green Construction and Smart Traffic Control of Transportation Infrastructure, Xinjiang University, Urumqi 830017, China

^b XINJIANG CONSTRUCTION & ENGINEERING GROUP CO.,LTD, 830000, China

^c National Engineering Laboratory of Highway Maintenance Technology, Changsha University of Science & Technology, Hunan 410114, China

^d Department of Civil and Environmental Engineering, The Hong Kong Polytechnical University, Hung Hom, Hong Kong

ARTICLE INFO

Keywords:

Road engineering
Subgrade
Self-weight effect
Bearing plate
Size effect
Modulus of resilience
Cyclic load simulation
Prediction model validation

ABSTRACT

This study investigates the impact of pavement structure self-weight on the dynamic and static resilient modulus of subgrade materials and proposes a prediction model to account for this effect. Traditional methods for measuring subgrade modulus are limited in simulating repeated traffic loading and the influence of self-weight, leading to inaccurate evaluations. To address this, a novel test device capable of applying cyclic loads was developed. Dynamic and static modulus tests were conducted using different bearing plate and lantern ring sizes to simulate the self-weight effect. Results show that the resilient modulus decreases as the bearing plate size increases, stabilizing at 30 cm, while the modulus increases with the collar size, stabilizing at 50 cm for a 20 cm plate and 35 cm for a 30 cm plate. A prediction model for dynamic and static resilient modulus, incorporating the effect of pavement self-weight, was developed. This model enhances the accuracy of subgrade modulus predictions, contributing to more reliable pavement structure designs. The findings are significant for improving the efficiency and accuracy of subgrade testing, with important implications for pavement design and maintenance.

1. Introduction

In pavement structure design, the subgrade resilience modulus represents the deformation resistance of subgrade and pavement. It is one of the most sensitive parameters affecting the thickness of the pavement structure layer and an important parameter for calculating subgrade and pavement load response. Subgrade resilience modulus is not only a mechanical index reflecting subgrade bearing capacity but also an important parameter for pavement structure design and subgrade completion acceptance. Therefore, the accurate and rapid determination of resilience modulus has significant engineering application value for Subgrade and pavement structure design, construction quality control, and maintenance decision-making[1–5].

In China's current code for 《Field Tests of Highway Subgrade and Pavement》(JTG 3450–2019)[6], the Beckmann beam

* Corresponding author at: National Engineering Laboratory of Highway Maintenance Technology, Changsha University of Science & Technology, Hunan 410114, China.

E-mail addresses: znt@xju.edu.cn (N. Zhang), wpeng@cscec.com (P. Wang), chengdong.xia@polyu.edu.hk (C. Xia), gaolingavin@126.com (L. Gao), wangyongz@cscec.com (Y. Wang), lst@csust.edu.cn (S. Lv), wdk281076719@outlook.com (W. Dikuan).

<https://doi.org/10.1016/j.cscm.2024.e04159>

Received 7 October 2024; Received in revised form 17 November 2024; Accepted 24 December 2024

Available online 26 December 2024

2214-5095/© 2024 The Authors. Published by Elsevier Ltd. This is an open access article under the CC BY-NC-ND license (<http://creativecommons.org/licenses/by-nc-nd/4.0/>).

deflectometer and bearing plate are mainly used to measure the deflection and resilience modulus of subgrade and pavement (Ministry of Transport of the People's Republic of China 2019). However, the Beckman beam and bearing plate methods are static detection methods that can only test subgrade and pavement's static deflection and modulus. Some problems, such as low test efficiency, poor convenience, prominent human influence factors, and large data dispersion, are challenging to meet the needs for accurate and rapid detection of highway engineering. In addition, the deflection and modulus of resilience test have always stipulated that Jiefang brand ca-10b and Huanghe brand Jn-150 are used as "standard vehicles" of two load levels. However, these two models are rarely used, which makes the "standard vehicles" unable to be standardized, resulting in different test results of different "standard vehicles" on the same pavement structure, which directly affects the accuracy and scientificity of subgrade and pavement deflection and modulus of resilience test. It is difficult to scientifically evaluate subgrade and pavement's structural resistance and load response.

In the 1950s and 1960s, the United States established an empirical formula between the bearing plate test results and the indoor test results through the full-scale ring road test years. The empirical formula can be used in pavement design. Many countries still adopt this result all over the world. In the 1960s and 1970s, China conducted a nationwide survey on the resilient modulus of subgrade and gave the recommended values of resilient modulus under various soil and climatic conditions for design use. However, because the test process of bearing plates is complex and time-consuming, countries worldwide have taken some flexible measures to obtain the resilient modulus of subgrade. In the 1980s, a drop weight deflectometer was developed, which simulates the traffic load with the impact load generated by the free fall of the heavy hammer on the bearing plate, and measures the deformation of the subgrade under the impact load through the displacement sensor. However, the test data is unstable, and the test reproducibility is not high. It is mainly used for pavement performance evaluation [7].

The subgrade resilience modulus testings mainly include indoor and outdoor tests. The indoor tests are mainly static triaxial tests and dynamic triaxial tests. Outdoor tests include the bearing plate method, Beckman beam method, falling weight deflectometer method (FWD), and portable falling weight deflectometer method (PFWD). Road researchers have carried out extensive research on obtaining the subgrade modulus.

Zhang et al. [8] combined a genetic algorithm for the inverse calculation of pavement modulus based on an artificial neural network and found that subgrade modulus is very important to the inverse calculation of pavement modulus. Jefferson Barbosa de Freitas et al. [9] found that the elastic modulus of the subgrade is an essential property to understanding pavement behavior, and elastic behavior is directly related to fatigue cracking and permanent deformation and proposed a model for predicting the elastic modulus of laterite and non-laterite tropical soils. Raja Abubakar Khalid et al. [10] studied the effect of overloaded weight on the resilience modulus of subgrade soil through the CBR test using the method of a heap load.

Weitian Zhao et al. [11] studied the structural state of cement concrete pavement based on bottom probing radar and FWD and found that the actual pavement performance is very different from the indoor performance. M.T. Cao-Rial et al. [12] found that the Rayleigh wave method can be used to obtain the material's elastic modulus, but it is necessary to obtain appropriate boundary conditions and initial conditions. Sajib Saha et al. [13] established a subgrade modulus response model by analyzing and correcting many FWD data.

Zulkuf Kaya et al. [14] studied the elastic modulus and shear modulus of soil through dynamic triaxial tests and found that the field modulus is significant for structural design. Ehsan Yaghoubi et al. [15] studied the performance of expansive soil treated with recycled glass through dynamic triaxial tests and found that the change of the subgrade modulus has a significant effect on the compressive and tensile strain in the pavement structure, which in turn affects the fatigue and rutting performance of the pavement. Gongfeng Xin et al. [16] studied the subgrade soil modulus under different confining pressure and moisture content through the dynamic triaxial test and found that the service performance of subgrade mainly depends on the dynamic elastic modulus of subgrade soil. Xiaolan Liu et al. [17] conducted triaxial tests to study the effects of stress level, loading frequency, etc., on the indoor dynamic and static elastic modulus and found that the static and dynamic elastic modulus were similarly affected. Hongguang Jiang et al. [18] carried out dynamic and static triaxial tests for medium and high liquid limit clays in the yellow flood zone. They found that the dynamic elastic modulus of the soil is generally higher than its static value, and the ratio of the two decays exponentially with the increase of the deviatoric stress ratio. Nasrin heidarabadizadeh et al. [19] found that the dynamic modulus of the resilience prediction model established based on the triaxial test was affected by many parameters such as confining pressure and deviatoric stress by analyzing the dynamic triaxial test data in the literature. Behnam Ghorbani et al. [20] established an elastic modulus prediction model of cohesive subgrade soil under a triaxial test based on a genetic algorithm to avoid dynamic triaxial tests requiring complex equipment and skilled operators. Ahmed S. El-Ashwah et al. [21] characterized the subgrade modulus by conducting triaxial tests considering the effects of stress state and moisture content.

Wangxi Zhang et al. [22] found that it is feasible to obtain the actual underground foundation parameters of the actual site through the load test of the bearing plate. Hong Shi [23] proposed the upper loading limit for on-site bearing plate tests suitable for different pavement structures by analyzing the relationship between subgrade stress and displacement under different pavement structures. Shutang Liu et al. [24] established a new formula for calculating the elastic modulus of soil based on the analysis of the elastic modulus of subgrade measured by the bearing plate method. Xiaoyong Li et al. [25] conducted a test of the bearing capacity of bearing plates of different sizes on the roadbed and found that the foundation coefficient has a size effect law. Prinya chinaprasirt et al. [26] Estimated the elastic modulus of on-site compacted loess through an indoor bearing plate test. The test shows that an indoor load test can estimate the on-site resilient modulus of loess.

By using FWD and Plate bearing testing on the base of rigid pavement, Fouzieh Rouzmehr et al. [27] analyzed the field deflection data and found that deflection-based quality assurance testing for support layers in PCC pavement is significantly different from traditional quality assurance testing. Also, there are some discrepancies between back-calculated (subgrade k-values and base modulus) and forward analysis (deflections) results, implying technical imperfections at this point.

In summary, the indoor triaxial test requires complex equipment and skilled personnel, and the measured results are different from

the field test results. The slight change in subgrade resilience modulus will significantly impact the design of the upper pavement structure, which makes the pavement design too wasteful or unsafe. The loading speed of the bearing plate method is slow, which is a static load; The impact load applied by the falling weight deflectometer is a one-time impact load. However, the actual subgrade is subjected to the repeated action of the moving traffic load and the self-weight load of the pavement. The load applied by the existing test methods is different from the load borne by the actual subgrade. The deformation response characteristics and resilient modulus of the subgrade obtained from the test can not truly reflect the anti-deformation characteristics of the subgrade.

At this stage, it is urgent to develop new test devices and methods for dynamic and static modulus of resilience of subgrade to more objectively reveal the behavior characteristics and evolution law of subgrade and pavement structure. In this paper, the self-developed combined test equipment of dynamic and static deflection and resilience modulus of subgrade and pavement with cyclic load is used to determine the influence of the size of the bearing plate on the dynamic and static modulus of subgrade by testing the dynamic and static resilience modulus of subgrade under different sizes of bearing plate ; In order to simulate the influence of the self-weight of pavement structure layer on the modulus of subgrade, the dynamic and static modulus of subgrade under different collar sizes were tested. The prediction model of dynamic and static modulus of subgrade considering the influence of the structural layer's self-weight is established to provide a reference for subgrade design and construction. This paper provides a basis for improving the effectiveness and reliability of asphalt pavement structure design and has particular theoretical and engineering application value.

2. Dynamic and static deflection and modulus of resilience testing equipment

2.1. Design ideas

In order to scientifically evaluate the structural resistance and load response of subgrade and pavement and more objectively reveal the behavior characteristics and evolution law of subgrade and pavement structure, joint test equipment of dynamic and static deflection and resilience modulus of subgrade and pavement with cyclic load is developed. The equipment is shown in Fig. 1.

2.2. Technical parameter

The dynamic and static loads are applied through the hydraulic servo device, and the pressure sensor is set to accurately control the size of the applied dynamic and static load. It is equipped with automatic acquisition and analysis software to analyze and process the test results without manual loading and reading, which realizes the automation and precision of the whole process of deflection and resilience modulus testing. It improves the test efficiency and the accuracy of test results. The main technical parameters of the equipment are shown in Table 1.

3. Overview of the test

3.1. Soil sample material

The low liquid limit clay is selected as the subgrade, and its technical indexes meet the requirements of code for the Test Methods of Aggregate for Highway Engineering (JTG / E42-2005)(Ministry of Transport of the People's Republic of China n.d.)[28].

According to the Test Methods of Soils for Highway Engineering (JTG-E3430-2020)(Ministry of Transport of the People's Republic of China n.d.)[29], the physical and mechanical property indexes of soil samples obtained from the test are shown in Table 2. During subgrade filling, the moisture content shall be controlled within the "optimum moisture content of - 3 % ~ + 2 %" as far as possible. The test shall be carried out immediately after compaction. The treated low-liquid limit clay foundation is shown in Fig. 2.

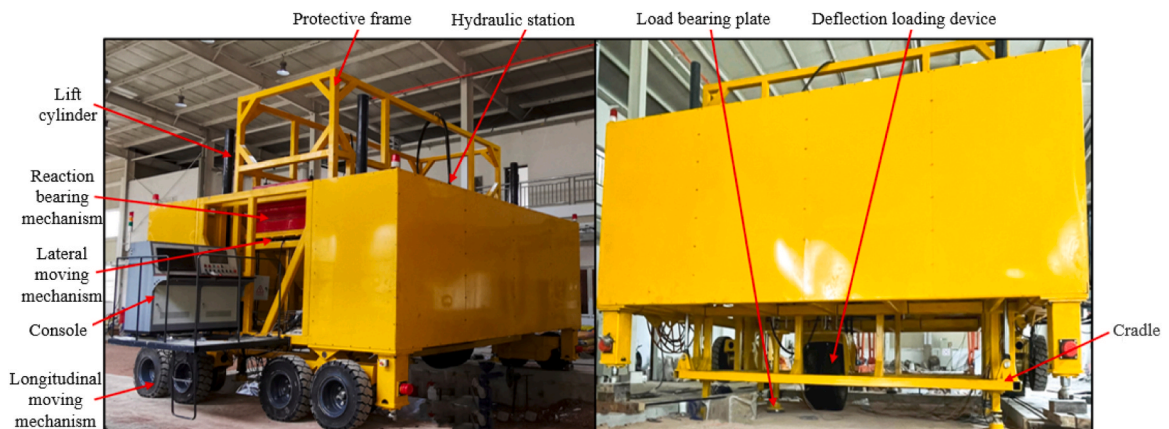


Fig. 1. Joint testing equipment for dynamic and static deflection and resilience modulus of subgrade and pavement.

Table 1
Main technical parameters of the equipment.

	Dynamic loading and unloading parameters	Static loading and unloading parameters		Displacement test parameters
Loading and unloading amplitude	0–50KN	0–120KN	Displacement amplitude range	0–20 mm
Loading and unloading accuracy	0.5KN	1KN	Displacement test accuracy	0.001 mm
Loading and unloading waveform	Sine wave, triangular wave, square wave, etc.	/	work environment	Temperature 0 ~ 40°C Humidity ≤ 80 %
Loading and unloading frequency range	0–15 Hz	/	The frequency range of displacement data acquisition	0–1000 Hz

Table 2
Physical parameters of clay with low liquid limit.

soil sample	Density /g·cm ³	Liquid limit /%	Plastic limit /%	Plasticity index /%	Optimum moisture content /%	Maximum dry density / g·cm ³
Low liquid limits clay	2.736	38.3	20.1	18.2	10.82	2.00

3.2. Test scheme

According to the "Field Test Methods of Subgrade and Pavement for Highway Engineering" (JTG 3450–2019)(Ministry of Transport of the People's Republic of China 2019), on the site soil surface, the joint test equipment for dynamic and static deflection and resilience modulus of subgrade and pavement is used for loading and the laser displacement sensor collects the whole process data.

Under static load, the subgrade is loaded and unloaded step by step through bearing plates of different sizes. The corresponding rebound deformation value of the subgrade under each load level is measured, and the rebound modulus of the subgrade is obtained through calculation. Use the test equipment to preload 0.05Mpa and stabilize the pressure for 1 min so that the bearing plate is in close contact with the subgrade. The equipment is controlled by step-by-step loading. The step-by-step loading gradient is 0.02 MPa before the load is less than 0.1 MPa, and 0.04 MPa after exceeding 0.1 MPa. After each loading to the predetermined load p , unload to 0 after stabilizing for one minute. After unloading and stabilizing for 1 min, continue to load to the next load level. The pressure on different collars applies fixed stress through a jack to simulate the influence of road self-weight load on the subgrade, and the pressure sensor is used to determine the force.

The dynamic resilient modulus is a measure of the subgrade material's ability to recover after being subjected to a cyclic loading or repeated traffic loads. It is determined during dynamic loading conditions, where the material undergoes repeated stress and strain cycles (such as those caused by moving vehicles).The static resilient modulus measures the subgrade material's stiffness under a single, non-repetitive load (static loading), without the unloading and reloading cycles associated with dynamic loading.

The dynamic load is determined by setting the vertical downward loading force in the test software, Setting the loading waveform in the test software, selecting the loading waveform as a semi-positive vector wave, and setting the loading frequency and repetition times in the test software. The standard test loading process is shown in Table 3. After the force, frequency, and repetition times of vertical downward loading are set, start the servo control system for test. The data acquisition system collects displacement(L_i), load (P_i), and corresponding loading frequency in real-time. The dynamic and static load loading and test process diagrams are shown in Fig. 3 and Fig. 4, respectively.



Fig. 2. Low liquid limits clay foundation.

Table 3
Number of repeated loading at each loading frequency.

Frequency (Hz)	Number of repetitions (times)
15	200
10	200
5	100
1	100

The bearing plate size: $\Phi 5\text{cm}$, $\Phi 10\text{cm}$, $\Phi 15\text{cm}$, $\Phi 20\text{cm}$, $\Phi 20\text{cm}$, $\Phi 30\text{cm}$, $\Phi 40\text{cm}$; The lantern ring sizes: internal diameter $\Phi 10\text{cm}$, outer ring width 15cm ; internal diameter $\Phi 20\text{cm}$, outer ring width in turn: 10cm , 15cm , 20cm , 25cm , 30cm , 40cm , 50cm , 60cm ; internal diameter $\Phi 30\text{cm}$, outer ring width in turn: 5cm , 10cm , 15cm , 20cm , 25cm , 35cm , 45cm , 55cm .

According to the stress and strain change data obtained from the test, calculate the equivalent static resilience modulus of subgrade (formula 1), equivalent static resilience modulus of subgrade (formula 2), and equivalent dynamic resilience modulus of subgrade (formulas 3, 4 and 5) under various loads according to the following formulas.

$$E_i = \frac{\pi D}{4} \cdot \frac{P_i}{L_i} (1 - \mu_0^2) \quad (1)$$

$$E_0 = \frac{\pi D}{4} \cdot \frac{\sum P_i}{\sum L_i} (1 - \mu_0^2) \quad (2)$$

$$\sigma_0 = \frac{P_i}{A} \quad (3)$$

$$\varepsilon_0 = \frac{\Delta_i}{l_0} \quad (4)$$

$$|E^*| = \frac{\sigma_0}{\varepsilon_0} \quad (5)$$

Where: E_i corresponds to the static modulus of resilience of subgrade under various loads (MPa); E_0 is the static modulus of resilience of subgrade (MPa); μ_0 is the Poisson's ratio of soil, which is taken according to relevant pavement design specifications; D is the diameter of bearing plate (cm); P_i is the pressure of bearing plate (MPa); L_i is the true rebound deformation of the corresponding load P_i (cm); σ_0 is axial stress amplitude (MPa); l_0 is the measurement spacing of the displacement sensor on the bearing plate (mm); ε_0 is the axial recoverable strain amplitude (mm/mm); Δ_i is the average amplitude of recoverable axial deformation in the loading cycle (mm); $|E^*|$ is the dynamic modulus of resilience of subgrade (MPa).

3.3. Influence quantity in subgrade test

The essence of total influence quantity is spring back deformation, an essential parameter to be determined in advance to determine

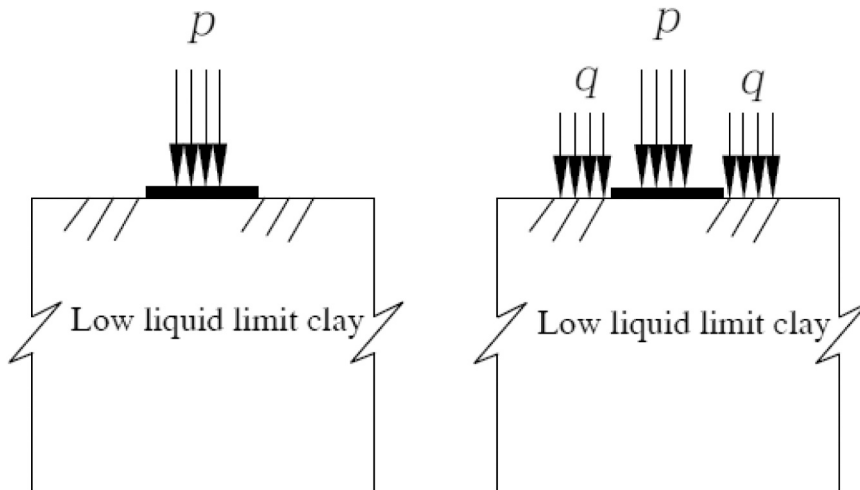


Fig. 3. Loading diagram.



Fig. 4. Test process diagram.

the grading influence quantity. It is produced by the axle load of the rear axle of the test vehicle acting on the subgrade and is located at the subgrade surface point corresponding to the center of the bearing plate in the deflection basin. 《Field test methods of highway subgrade and pavement》(JTG 3450–2019)(Ministry of Transport of the People's Republic of China 2019) stipulate its size as the average difference between two dial indicators' initial and final readings. In practical terms, this is not accurate. The equipment selects the sum of the difference between the initial and final readings of the laser sensor placed before and after the subgrade as its size[24].

The total influence quantity is expressed by a , which is the rebound deformation produced by the equipment axle load acting on the subgrade at the bearing plate when the loading axle has no jacking effect on the test equipment. Set the equipment weight as Q . when loading P_i ($i = 1, 2, \dots, n$) in stages, the load of the equipment support shaft acting on the subgrade surface is reduced due to the upward jacking effect of the loading shaft. The reduced load also has a corresponding influence amount (rebound deformation), but the influence amount is no longer a and is set as A_i ; A_i can be obtained through analysis. The problem of graded influence A_i occurs in the analysis process.

Under the assumption of elastic half-space, the rebound deformation of the subgrade is directly proportional to the load acting on the subgrade surface by the loading axis. Therefore, the rebound deformation A_i generated by force W_i between the loading axis and subgrade at the bearing plate is:

$$A_i = \frac{w_i}{Q} a = a - \frac{T_1 + T_2}{4T_1 Q} \pi D^2 p_i a \quad (6)$$

Then the classification influence amount a_i under all levels of pressure is:

$$a_i = \frac{T_1 + T_2}{4T_1 Q} \pi D^2 p_i a \quad (7)$$

Where: T_1 is the wheelbase in front of the equipment loading shaft (m); T_2 is the wheelbase after the equipment is loaded (m); D is the diameter of the bearing plate (m); Q is the weight of test equipment (N); P_i is the pressure of bearing plates at all levels (Pa); a is the total influence amount (0.01 mm).

The load-deformation coordinate system determines whether a straight line passes through the origin. Therefore, when using this formula to calculate the modulus of resilience, to ensure the use conditions of the formula, it is necessary to modify the coordinate origin to make the drawn curve initially pass through the origin of the new coordinate system.

Eq. (2) is an analytical formula of elastic modulus based on the ideal elastic half-space model. Therefore, the actual spring back deformation generated by the load P_i must be the measured spring back deformation L_i plus the corresponding graded influence a_i , the corresponding load. The accurate spring back deformation of P_i is $L_i = l_i + a_i$.

In this study, the dynamic and static loading tests under the different bearing plate and collar sizes are carried out to establish the relationship between the dynamic and static elastic modulus characteristics of subgrade and the size of the bearing plate and collar.

4. Test results and analysis

4.1. Test results under different bearing plate sizes

Firstly, the static loading tests of bearing plates with different sizes are carried out to study the relationship between the characteristics of static resilience modulus and the size of bearing plates. The equivalent resilience modulus of subgrade top surface of bearing plates with different sizes under static load is shown in Fig. 5.

It can be seen from Fig. 5 that the change of equivalent resilient modulus of subgrade top surface is negatively correlated with the change of bearing plate size. The value of equivalent resilient modulus decreases with the increase of bearing plate size. The size of the

bearing plate increases to a certain extent ($\Phi 30$ cm), and the change of equivalent resilient modulus of subgrade top surface tends to be stable and close to a particular limit value.

It shows that with the increase of the load area, the subgrade will produce partial plasticity based on elastic deformation, making the measured modulus of resilience gradually smaller. Due to the different sizes of bearing plates, the measured modulus values under different sizes are different, affecting the pavement structure design.

Under the action of dynamic load, the equivalent resilience modulus of subgrade top surface under different sizes of bearing plates and different frequencies is shown in Fig. 6.

It can be seen from Fig. 6 that the equivalent dynamic resilience modulus of subgrade top surface under different bearing plate sizes decreases with the increase of bearing plate size. It shows that the variation law of equivalent resilient modulus of subgrade top surface under dynamic and static load is the same, negatively correlated with the change of bearing plate size. Under the identical size of the bearing plate, the equivalent dynamic resilience modulus of the subgrade top surface increases with the increase of loading frequency. The dynamic resilience modulus of each bearing plate size is fitted under different loading frequencies. The fitting diagram is shown in Fig. 7.

It can be seen from Fig. 7 that the dynamic resilient modulus of bearing plates with different sizes under different loading frequencies can be fitted by the Boltzmann function, and the correlation is high. The dynamic resilient modulus of bearing plates with different sizes under different frequencies can be estimated according to the fitting equation. See Table 4 for the dynamic resilience modulus fitting equation parameters under each bearing plate size.

4.2. Test results under different lantern ring sizes

In order to simulate the influence of self-weight of the pavement structure layer, the thickness of the pavement structure layer is 74 cm, and the density is 2.3 g/cm^3 . The calculated pressure of the pavement structure layer is 0.017 MPa. Use the jack to apply the reaction force, and determine the force through the pressure sensor. Fig. 8 shows the static modulus of elasticity of the top surface of the subgrade under the same collar width of the bearing plate $\Phi 10$ cm, $\Phi 20$ cm, and $\Phi 30$ cm.

It can be seen from Fig. 5 that under the same collar width, the increase of static resilience modulus of the bearing plate is close. It can be seen from Fig. 5 that the subgrade modulus begins to converge when the bearing plate is $\Phi 30$ cm, so the following paper mainly studies the bearing plates $\Phi 20$ cm and $\Phi 30$ cm. When the pressure changes, the actual spring back deformation of the $\Phi 20$ cm and $\Phi 30$ cm bearing plates under different collar sizes are shown in Fig. 9 and Fig. 10.

It can be seen from Fig. 9 and Fig. 10 that the actual spring back deformation under the $\Phi 20$ cm and $\Phi 30$ cm bearing plates both increases with the increase of the bearing plate pressure and decreases with the increase of the size of the collar. The above test shows that the actual rebound deformation and rebound modulus have slight fluctuation under the joint test equipment of dynamic and static deflection and rebound modulus. The discreteness is obviously smaller than that of the traditional test method.

The elastic modulus of the subgrade top surface of the $\Phi 20$ cm and $\Phi 30$ cm bearing plates under different collar sizes see Fig. 11 and Fig. 12.

It can be seen from Fig. 11 that under different collar sizes of the $\Phi 20$ cm bearing plate, the static elastic modulus of the bearing plate increases with the increase of the collar size. When the collar width increases to 50 cm, the influence of the static modulus of elasticity begins to stabilize gradually.

It can be seen from Fig. 12 that the variation law of the $\Phi 30$ cm bearing plate is the same as that of the bearing plate $\Phi 20$ cm under different collar sizes when the collar width increases to 35 cm, the static elastic modulus of the top surface of the subgrade begins to stabilize. A fitting equation is established through regression analysis of the test data, as shown in Eqs. 8 and 9. Whether the bearing

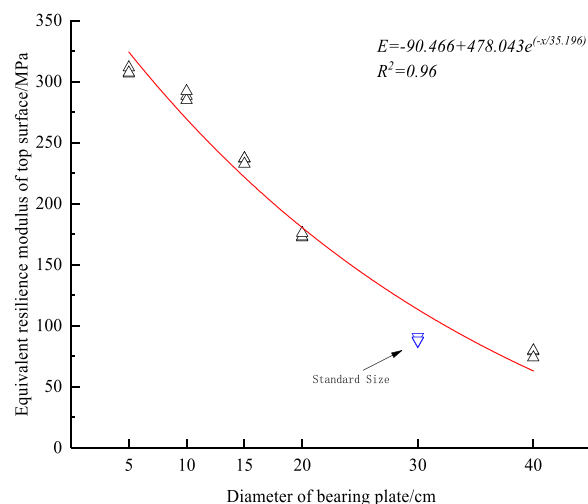


Fig. 5. Equivalent resilient modulus of the top surface of subgrade with bearing plates of different sizes under static load.

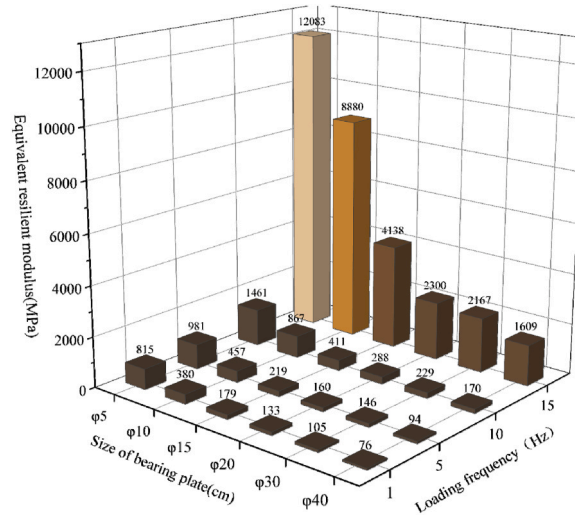


Fig. 6. Equivalent resilient modulus of the top surface of subgrade with different bearing plate sizes under dynamic load.

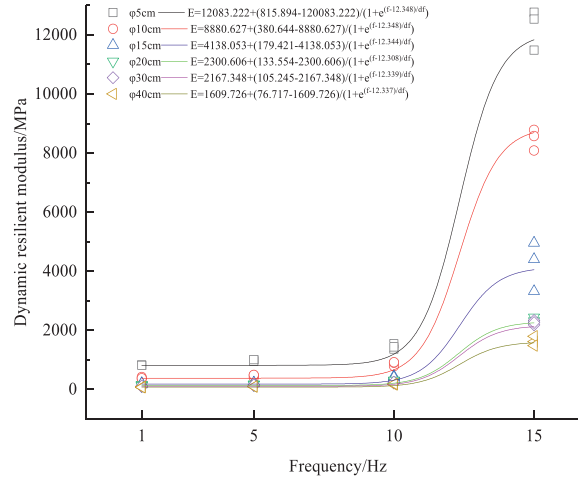


Fig. 7. The fitting diagram of equivalent resilient modulus of subgrade top surface with different bearing plate sizes under dynamic load.

Table 4

Main curve fitting function parameters of bearing plates with different sizes.

Fitting equation	$ E^* = A_2 + \frac{A_1 - A_2}{1 + e^{(f-f_0)/df}}$				
Fitting parameters	A_1	A_2	f_0	df	R^2
Bearing plate φ5 cm	815.89	12083.22	12.35	0.7	0.99
Bearing plate φ10 cm	380.64	8880.63	12.35	0.7	0.99
Bearing plate φ15 cm	179.42	4138.05	12.34	0.7	0.99
Bearing plate φ20 cm	133.55	2300.61	12.31	0.7	0.99
Bearing plate φ30 cm	105.25	2167.35	12.4	0.7	0.99
Bearing plate φ40 cm	76.72	1609.73	12.34	0.7	0.99

plate is φ20 cm or φ30 cm, the correlation is good. This formula can predict the static resilient modulus of the subgrade top surface under different collar sizes and realize the conversion between the traditional test results and the static resilient modulus of the subgrade top surface considering the road weight.

$$E_{20} = 162.8 - \frac{34.4}{\left(1 + (x/34.3)^{0.6}\right)} R^2 = 0.96 \quad (8)$$

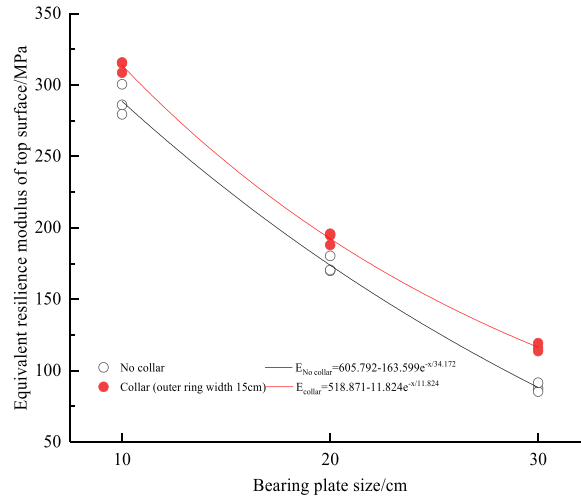


Fig. 8. Static resilient modulus of subgrade top of $\Phi 10$ cm, $\Phi 20$ cm, $\Phi 30$ cm bearing plates under the same collar width.

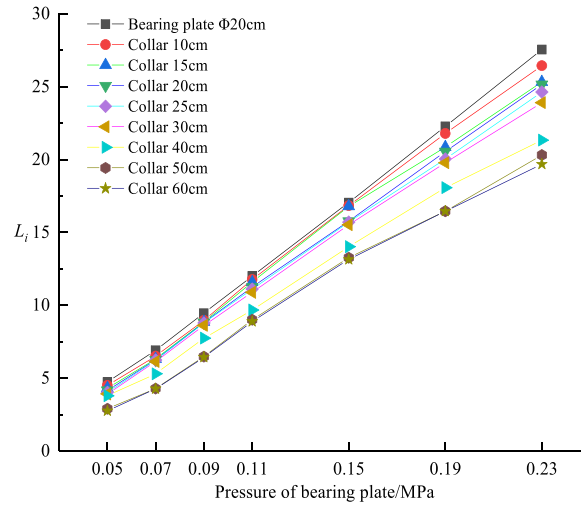


Fig. 9. The actual spring back deformation diagram of the subgrade top surface under different ring sizes of the bearing plate $\Phi 20$ cm when the pressure changes.

$$E_{30} = 107.7 - \frac{19.1}{\left(1 + (x/21.2)^{3.3}\right)} R^2 = 0.99 \quad (9)$$

Where: E_{20} is the static resilient modulus of the subgrade top surface of the bearing board $\Phi 20$ cm (MPa); E_{30} is the static resilient modulus of the subgrade top surface of the bearing board $\Phi 30$ cm (MPa); x is the outer ring width of the collar (cm).

Comparing Fig. 11 and Fig. 12, it can be seen that the convergence of the $\Phi 30$ cm bearing plate is better than that of the $\Phi 20$ cm bearing plate. According to the above research results, in order to simulate the influence of the weight of the pavement structure layer, the test results are the most stable when the bearing plate is $\Phi 30$ cm, the outer ring width of the collar is 45 cm (the inner diameter of the collar is $\Phi 30$ cm, and the outer diameter is $\Phi 60$ cm).

In order to solve the problem that the size of the collar is too large and it is inconvenient to use, different loads are applied to the same collar size (the bearing plate is $\Phi 30$ cm, and the collar width is 20 cm). The influence of the change of the collar load on the modulus of the bearing plate is studied. The test results are shown in Fig. 13.

It can be seen from Fig. 13 that the bearing plate is $\Phi 30$ cm, and the collar is 20 cm wide. Under different collar loads, the static resilient modulus of the top surface of the subgrade increases with the increase of the load. When the load reaches 0.06 MPa, the static resilient modulus of the top surface of the subgrade reaches 104 MPa, which is close to the convergence value when the collar size is 35 cm.

Therefore, the small-size collar can be used to increase the load and realize the effect of simulating the self-weight of the pavement

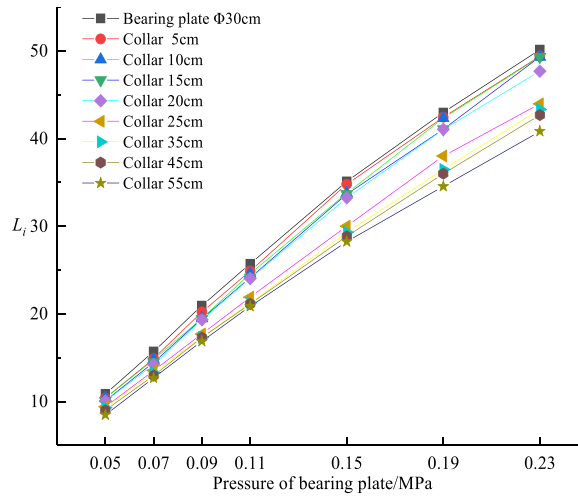


Fig. 10. The actual spring back deformation diagram of the subgrade top surface under different ring sizes of the bearing plate $\Phi 30$ cm when the pressure changes.

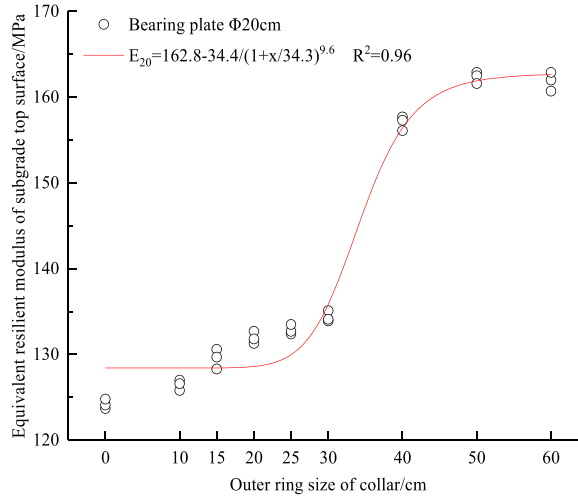


Fig. 11. The static resilient modulus diagram of the top surface of the subgrade under different collar sizes of the $\Phi 20$ cm bearing plate.

structure layer.

Fig. 14 and Fig. 15 show the dynamic resilient modulus of $\Phi 20$ cm and $\Phi 30$ cm bearing plates at different frequencies and collar sizes.

It can be seen from Fig. 14 and Fig. 15 that under the action of dynamic load, the dynamic resilient modulus increases with the increase of the collar size. When the ring width increases to a certain extent, the change of the dynamic resilient modulus of subgrade tends to be stable and close to a particular limit value. When the collar size is the same, the dynamic resilience modulus of the subgrade top surface increases with the increase of loading frequency. When the bearing plate is $\Phi 20$ cm, the dynamic modulus value tends to be stable when the ring width is 50 cm; when the bearing plate is $\Phi 30$ cm, the dynamic modulus value tends to be stable when the ring width is 35 cm. Consistent with the static load effect, the test results under different collar sizes are consistent.

The dynamic modulus of the bearing plate $\Phi 30$ cm, the collar width of 35 cm, and the bearing plate $\Phi 20$ cm collar width of 50 cm are fitted, and the fitting curve is shown in Fig. 16.

It can be concluded from Fig. 16 that the dynamic elastic modulus of different sizes of bearing plates and different sizes of collars under different loading frequencies can be fitted by the Boltzmann function, and the correlation is high. Through fitting, the estimated equations of dynamic resilience modulus under the condition that the bearing plate $\Phi 30$ cm collar width is 35 cm and the bearing plate $\Phi 20$ cm collar width 50 cm are obtained. The fitting equations are shown in Eqs. 10 and 11. According to this model, it is possible to estimate the dynamic resilient modulus of the subgrade top surface considering the influence of the self-weight of the pavement structural layer under different frequencies of a specific bearing plate size.

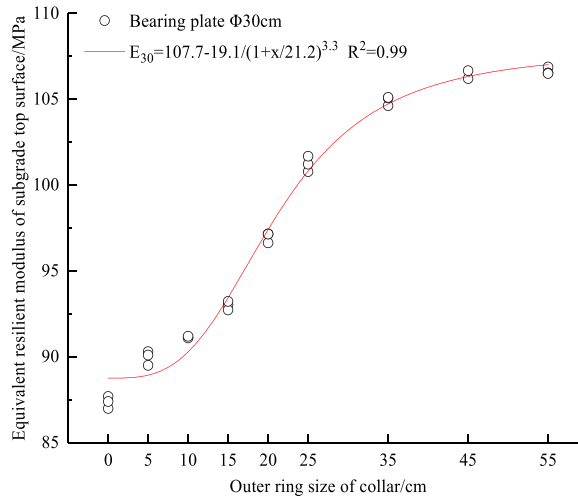


Fig. 12. The static resilient modulus diagram of the top surface of the subgrade under different collar sizes of the $\Phi 30$ cm bearing plate.

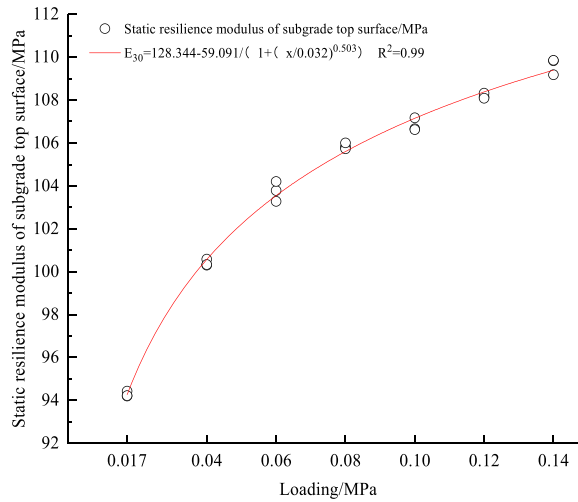


Fig. 13. The influence of the change of the collar load on the modulus of the bearing plate (the bearing plate is $\Phi 30$ cm, and the collar width is 20 cm).

$$E_{20d} = 2337 - \frac{2165}{(1 + e^{(f-12.306)/df})} R^2 = 0.99 \quad (10)$$

$$E_{30d} = 2184 - \frac{2062}{(1 + e^{(f-12.339)/df})} R^2 = 0.99 \quad (11)$$

Where: E_{20d} is the dynamic resilience modulus of the subgrade top surface of the bearing board $\Phi 20$ cm (MPa); E_{30d} is the dynamic resilience modulus of the subgrade top surface of the bearing board $\Phi 30$ cm (MPa); f is the loading frequency (Hz).

5. Conclusions

In order to consider the influence of the self-weight of the pavement structure layer on the dynamic and static modulus of the subgrade and establish a more accurate dynamic and static modulus prediction model, this paper reveals the dynamic and static elastic modulus changes of the subgrade under different bearing plate sizes and different collar sizes. On this basis, a prediction model of soil resilience modulus was established. The main conclusions are as follows:

- (1) Through the actual measurement and result analysis of the dynamic and static test of subgrade bearing plate, the feasibility of the joint test equipment of dynamic and static deflection and resilience modulus is verified. The equipment is loaded with cyclic

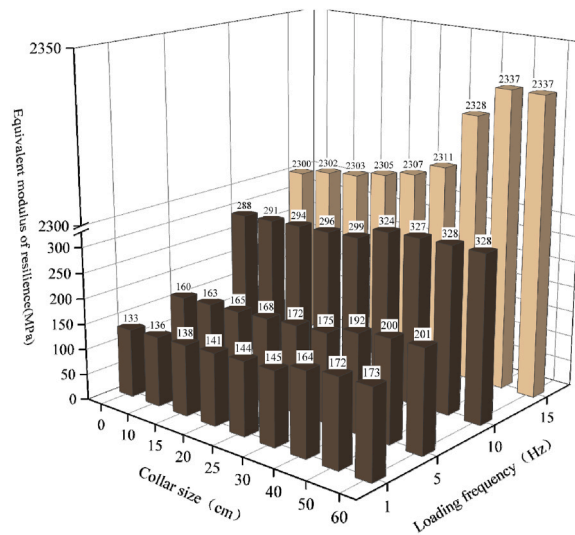


Fig. 14. Dynamic resilient modulus diagram of subgrade top surface under different collar sizes of $\Phi 20$ cm bearing plate.

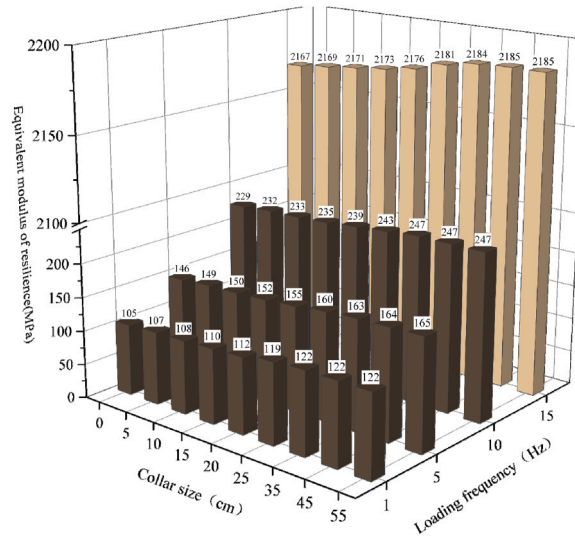


Fig. 15. Dynamic resilient modulus diagram of subgrade top surface under different collar sizes of $\Phi 30$ cm bearing plate.

load, high test accuracy, easy implementation, and strong operability. It is closer to the actual stress condition of the subgrade and is suitable for rapid detection of subgrade.

- (2) The modulus of elasticity of the roadbed is closely related to the bearing plate's size and the collar's size. Whether or not to consider the influence of the road surface weight has a significant influence on the measured elastic modulus of the roadbed. The dynamic and static resilience modulus of subgrade gradually decreases with the increase of the size of the bearing plate and becomes stable when the size reaches 30 cm. The dynamic and static resilient modulus of subgrade increase gradually with the increase of collar size. When the bearing plate is $\Phi 20$ cm, the size of the collar begins to stabilize when it reaches 50 cm; when the bearing plate is $\Phi 30$ cm, the collar begins to converge when the size reaches 35 cm.
- (3) The relationship between the bearing plate and collar size and the dynamic and static modulus of resilience of the subgrade top surface is obtained. The corresponding prediction model of modulus of resilience is established. The dynamic and static elastic modulus prediction model proposed in this paper has a high reference value for predicting the resilient modulus of Subgrade in the actual structure.
- (4) In this paper, only the on-site resilient modulus test of the subgrade is carried out, and the corresponding indoor dynamic and static triaxial test should be followed up to study the relationship between indoor dynamic and static resilient modulus and on-site dynamic and static resilient modulus.

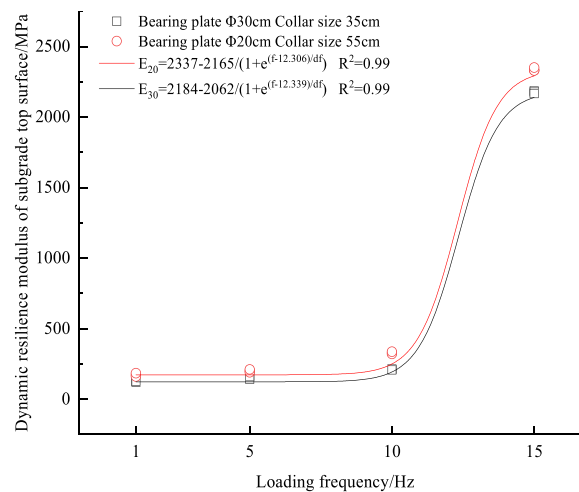


Fig. 16. The fitting curve of dynamic resilience modulus of subgrade top surface under specific collar width of bearing plate Φ30 cm and bearing plate Φ20 cm.

CRedit authorship contribution statement

Peng Wang: Validation, Data curation. **Chengdong Xia:** Writing – review & editing, Validation, Supervision. **Naitian Zhang:** Writing – original draft, Methodology, Investigation. **Songtao Lv:** Writing – review & editing, Supervision. **Wang Dikuan:** Writing – review & editing. **Lin Gao:** Resources, Investigation. **Yongze Wang:** Validation, Supervision.

Declaration of Competing Interest

The authors declare that they have no known competing financial interests or personal relationships that could have appeared to influence the work reported in this paper.

Acknowledgments

This work was supported by the National Natural Science Foundation of China (52225806 , 51608058 , 51927814), Youth Science Foundation of Xinjiang Uygur Autonomous Region Natural Science Foundation (2024D01C251), Basic scientific research projects of universities in Xinjiang Uygur Autonomous Region (202435120001) , Open Fund of Key Laboratory of Special Environment Road Engineering of Hunan Province (kfj230602, kfj230205)

Data availability

Data will be made available on request.

References

- [1] E. Sadrossadat, A. Heidarianpanah, S. Osouli, Prediction of the resilient modulus of flexible pavement subgrade soils using adaptive neuro-fuzzy inference systems, *Constr. Build. Mater.* 123 (2016) 235–247.
- [2] L. Yu, J. Xie, R. Li, J. Hu, J. Pei, Study on the performance of emulsified asphalt recycled subgrade based on the evaluation of semi-rigid milling material, *Constr. Build. Mater.* 324 (2022) 126614.
- [3] W. Gong, L. Zuo, L. Li, H. Wang, Prediction of stratified ground consolidation via a physics-informed neural network utilizing short-term excess pore water pressure monitoring data, *Comput. -Aided Civ. Infrastruct. Eng.* (2024).
- [4] L.L. Pengli Ren, Zhang-Long Chen, Weibing Gong, Jingpei Li, Dynamic responses of a rough road comprising dry and saturated layers subjected to moving-vibratory elliptical traffic load: insights from a GMM-based semi-analytical solution, *Comput. Geotech.* 172 (2024) 106403.
- [5] Z.-L.C. Pengli Ren, Lin Li, Weibing Gong, Jingpei Li, Dynamic shakedown behaviors of flexible pavement overlying saturated ground under moving traffic load considering effect of pavement roughness, *Comput. Geotech.* 168 (2024) 106134.
- [6] M.o.T.o.t.P.s.R.o, China., Field test methods of highway subgrade and pavement, China Communications Press, Beijing, 2019.
- [7] N. Kheradmandi, A. Modarres, Precision of back-calculation analysis and independent parameters-based models in estimating the pavement layers modulus-Field and experimental study, *Constr. Build. Mater.* 171 (2018) 598–610.
- [8] X. Zhang, F. Otto, M. Oeser, Pavement moduli back-calculation using artificial neural network and genetic algorithms, *Constr. Build. Mater.* 287 (2021) 123026.
- [9] J.B. de Freitas, L.R. de Rezende, G. de FN Gitirana Jr, Prediction of the resilient modulus of two tropical subgrade soils considering unsaturated conditions, *Eng. Geol.* 270 (2020) 105580.
- [10] R.A. Khalid, N. Ahmad, M.U. Arshid, S.B. Zaidi, T. Maqsood, A. Hamid, Performance evaluation of weak subgrade soil under increased surcharge weight, *Constr. Build. Mater.* 318 (2022) 126131.
- [11] W. Zhao, Q. Yang, W. Wu, J. Liu, Structural condition assessment and fatigue stress analysis of cement concrete pavement based on the GPR and FWD, *Constr. Build. Mater.* 328 (2022) 127044.

- [12] M.T. Cao-Rial, C. Moreno, P. Quintela, Determination of young modulus by using rayleigh waves, *Appl. Math. Model.* 77 (2020) 439–455.
- [13] S. Saha, F. Gu, X. Luo, R.L. Lytton, Development of a modulus of subgrade reaction model to improve slab-base interface bond sensitivity, *Int. J. Pavement Eng.* 21 (14) (2020) 1794–1805.
- [14] Z. Kaya, A. Erken, Cyclic and post-cyclic monotonic behavior of Adapazari soils, *Soil Dyn. Earthq. Eng.* 77 (2015) 83–96.
- [15] E. Yaghoubi, M. Yaghoubi, M. Guerrieri, N. Sudarsanan, Improving expansive clay subgrades using recycled glass: resilient modulus characteristics and pavement performance, *Constr. Build. Mater.* 302 (2021) 124384.
- [16] G. Xin, A. Zhang, Z. Wang, Q. Shen, M. Mu, Influence of humidity state on dynamic resilient modulus of subgrade soils: considering repeated wetting-drying cycles, *Adv. Mater. Sci. Eng.* 2021 (1) (2021) 3532935.
- [17] X. Liu, X. Zhang, H. Wang, B. Jiang, Laboratory testing and analysis of dynamic and static resilient modulus of subgrade soil under various influencing factors, *Constr. Build. Mater.* 195 (2019) 178–186.
- [18] H. Jiang, S. Chen, H. Sun, Dynamic and static resilient modulus and their prediction models of medium-high liquid limit clay in yellow river flooded areas, China *J. Highw. Transp.* 34 (3) (2021) 103–112.
- [19] N. Heidarabadizadeh, A.R. Ghanizadeh, A. Behnood, Prediction of the resilient modulus of non-cohesive subgrade soils and unbound subbase materials using a hybrid support vector machine method and colliding bodies optimization algorithm, *Constr. Build. Mater.* 275 (2021) 122140.
- [20] B. Ghorbani, A. Arulrajah, G. Narsilio, S. Horpibulsuk, M.W. Bo, Hybrid formulation of resilient modulus for cohesive subgrade soils utilizing cpt test parameters, *J. Mater. Civ. Eng.* 32 (9) (2020) 06020011.
- [21] A.S. El-Ashwah, A.M. Awed, S.M. El-Badawy, A.R. Gabr, A new approach for developing resilient modulus master surface to characterize granular pavement materials and subgrade soils, *Constr. Build. Mater.* 194 (2019) 372–385.
- [22] W. ZHANG, B. CHEN, L. XIAO, J. Liu, X. DENG, Experimental study and evaluation methodology of foundation coefficients for two-parameter foundation model based on rigid plate loading tests, *J. Hunan Univ.* 45 (9) (2018) 122–129.
- [23] H. SHI, Research on test method for modulus of resilience bearing plates on highway soil roadbed, *Technol. Highw. Transp.* 04 (2011) 1–4. + 13.
- [24] S. Liu, W. Cao, Y. Li, J. Fang, Key technique and new calculating method for resilient modulus of subgrade measured by bearing plate, *China J. Highw. Transp.* 27 (2014) 23–29.
- [25] X.Y. Li, K. Xu, S.Y. Wang, Experimental study on size effect of plate load test in roadbed compaction quality detection, *Adv. Mater. Res.* 230 (2011) 367–371.
- [26] P. Chindaprasirt, A. Sriyotatch, A. Arngbunta, P. Chetchotisak, P. Jitsangiam, Estimation of modulus of elasticity of compacted loess soil and lateritic-loess soil from laboratory plate bearing test, *Case Stud. Constr. Mater.* 16 (2022) e00837.
- [27] F. Rouzmehr, P. Choi, J.H. Nam, M. Won, Improvements of quality assurance testing program for subgrade and base layer construction, *Constr. Build. Mater.* 310 (2021) 125157.
- [28] M.o.T.o.t.P.s.R.o.C. n.d, *Test Methods of Aggregate for Highway Engineering*, Beijing : China Communications Press.
- [29] M.o.T.o.t.P.s.R.o.C. n.d, *Test Methods of Soils for Highway Engineering*, Beijing : China Communications Press.